Numerical analysis for the influence of the construction of the secondary reaction plate on the characteristics of linear induction motor

- for urban rail-guided transportation -

NINH VAN CUONG, TAKAFUMI KOSEKI
Department of Electrical Engineering
The University of Tokyo
Tokyo, Japan
ninh.cuong@koseki.t.u-tokyo.ac.jp
takafumikoseki@ieee.org

EISUKE ISOBE
Japan Subway Association
Tokyo, Japan
isobe@jametro.or.jp

***Abstract*—In Linear Induction Motor for rail-guided transportation, to meet the demand for reducing transverse edge-effect and correspond to the end ring of rotary induction motor, various types of the construction of secondary reaction plate have been considered. In order to demonstrate the characteristics of each model, this paper describes the fundamental mathematical formulation of the simplified field calculation as well as the simulation results through 3-dimensional numerical analysis.**

Keywords—Linear Induction Motor, end-effect, edge-effect, secondary reaction plate, 3D numerical analysis

I. INTRODUCTION

It is a requirement in urban transportation systems to reduce construction, maintenance, and operation costs, improve comfort and convenience, as well as to be friendly with the environment. Japanese companies have been working on the development of the Linear Metro since the 1970s in order to meet these requirements. Driven by a Linear Induction Motor (LIM) and employing a steel wheel/steel rail track system, the Linear Metro is an advanced urban transportation system offering a wide range of features that are not available in other train systems [1].

However, in comparison with traditional driven systems, LIM driven system has lower efficiency and power factor because LIM has special characteristics and inherent problems due to the non-continuity of the magnetic field. Longitudinal end-effect and transverse edge-effect are two major electromagnetic phenomena of LIM, which makes the analysis, design and control of this motor difficult [2].

It is difficult to carry out the experiments for analysis and design of LIM due to the features of construction requirements. Although two-dimensional (2-D) analysis cannot express the influence of transverse edge-effect caused by the finite widths of the electromagnetic problem, still a few researchers have applied them in analyzing problems of LIM but not 3-D methods because 3-D methods are too complicated and they require a substantial computer memory and very long computation time.

In this paper, from fundamental mathematics and formulation of the simplified field calculation, by using 3-D numerical analysis, the influence of the finite length of the primary part and the finite width of the secondary part will be considered in LIM performance. For high performance consideration, the model of LIM with cap for secondary reaction plate has been presented.

II. LIM MODEL AND ITS PROBLEMS

A. Analysis Model

The side view of analysis model based in LIM for linear metro system in Japan with both the front view and the construction of the one-coiled phase are presented in Fig. 1. In addition, design parameters and analysis conditions are indicated in Table 1 and Table 2.

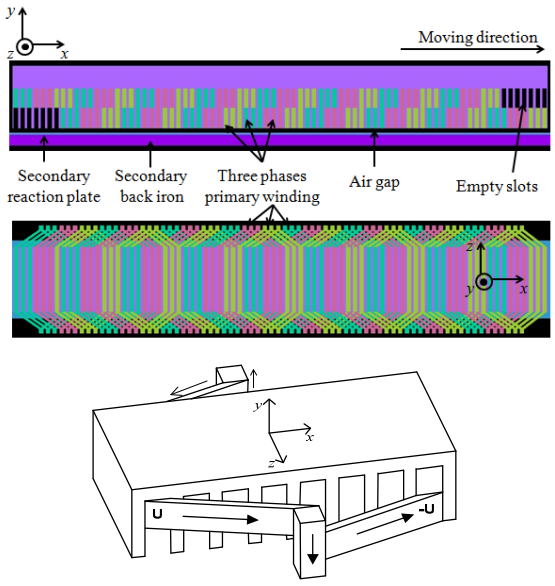

Fig. 1. Model of LIM based on linear metro in Japan.

TABLE I
Design Parameters of LIM for linear metro

Name	Parameter	Symbol	Value
Primary	Primary current	I_1	208A
	Motor length	L	2.476m
	Number of phases	m	3
	Number of poles	p	8
	Pole pith	τ	280.8 mm
	Stack hight	h	300 mm
	Core hight	d_a	124 mm
	Slot pitch	t_s	31.2 mm
	Slot width	w_s	20 mm
	Slot depth	d_s	79.5 mm
	Tooth width		11.2 mm
	Coil pitch	β	7/9
	Number of turn/phase	N	9
Secondary	Mechanical clearance	g	12 mm
	Thichness of back iron	d_1	22 mm
	Thickness of reaction plate	d_2	5 mm
	Overhang length	c	30 mm
	Secondary conductor width	h_2	360 mm

TABLE II
The Analysis Conditions

Parameter	Value
Primary frequency [Hz]	21
Synchronous speed [km/h]	42.3
Relative permeability in primary/back iron	1000
Conductivity in primary/back ion [S/m]	0
Material of conduction plate	Cu

B. LIM Problems Relating Edge Elements

- *Edge Effect*

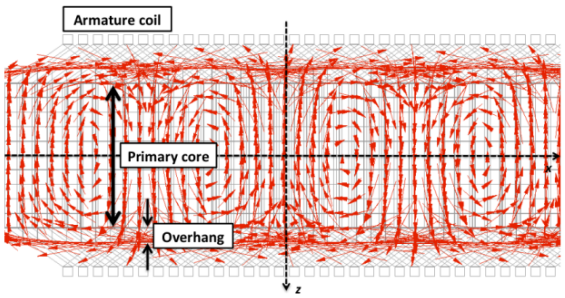

Fig. 2. Distribution of eddy currents in secondary reaction plate

The thrust of LIM is generated by the combination between the air gap magnetic flux and the eddy current that follows the perpendicular of moving direction in the secondary reaction plate. However, since LIM has the finite width of the secondary reaction plate, at the periphery of the plate, the current wrap occurs, as shown in Fig. 2. Therefore, when eddy currents flow in other parts of the product thickness direction, the current component is not involved in generating thrust. As a result, the transverse edge effect is a factor that has some influence on the effective secondary current and also on motor performance.

- *Difficult Points on Eddy Current Analysis*

To solve the problems on eddy currents, together with the implementation of the secondary back ion, the construction of secondary reaction plate is also an important design field. Therefore, based on the electromagnetic field analysis, it is necessary to evaluate the influence of electromagnetic field on cross-section shape of conductor and implementation core.

However, what kind of shape can be taken in electromagnetic analysis is a difficult question. Conventional analysis technique can be used for electromagnetic field analysis in two axes: height direction and travel direction. According to the effect of eddy currents in general and the effect of edge-effect in particular, the analysis of current distribution of the product thickness direction is necessary but it is impossible to be conducted in conventional analysis. Although 3-D analysis provides more accurate results than 2-D analysis does, the electromagnetic equation must be described in three coordinate components. Hence, in 3-D analysis, computational cost becomes bigger. Furthermore, it is impossible to set the periodical boundary conditions to consider the influence of edge effect. Even if you apply the periodical boundary conditions by ignoring the edge-effect temporarily, computation time will be enormous in case of LIM. Therefore; this method cannot be practiced in many cases of the secondary shape.

III. 3-D TRANSIENT ANALYSIS FOR LIM

A. 3-D Transient Magnetic Field Analysis with Edge Elements

The equation to represent the performance of LIM with eddy current is formulated as follow [3][4][5]:

$$\nabla\times\{\upsilon(\nabla\times\mathbf{A})\}=\mathbf{J}_0+\mathbf{J}_e \tag{1}$$

where J_e can be obtained from Maxwell equation as

$$\mathbf{J}_e=\sigma(\mathbf{E}_e+v\times\mathbf{B}) \tag{2}$$

or

$$\mathbf{J}_e=\sigma(-\frac{\partial\mathbf{A}}{\partial t}-\nabla\phi+v\times(\nabla\times\mathbf{A})) \tag{3}$$

where

υ is the magnetic resistivity,
$\mathbf{A}$ is the magnetic vector potential,
$\mathbf{J}_0$ is the exciting current density,
$\mathbf{J}_e$ is the eddy current density,
$\mathbf{E}_e$ is the electric field by eddy current,
$\mathbf{B}$ is the magnetic flux density,
v is the moving speed of the conductor,
σ is the conductivity, and
ϕ is the electric scalar potential.

In order to consider the influence of edge element, the electric scalar potential ϕ must be taken into account. The thrust of armature can be obtained by the Maxwell stress tensor method.

B. Induced Voltage Calculation

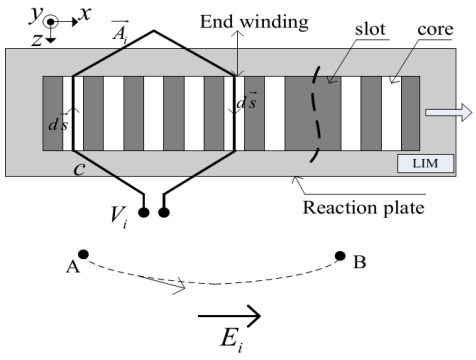

Fig. 3. Assumption of integral route in line integral of magnetic vector potential.

Magnetic vector potential can be obtained through numerical analysis, so from Maxell equation, the inter-linkage flux Φ of the exciting coil can be determined by direct integration over the coil length of the distribution of magnetic vector potential $\mathbf{A}$ as [5]:

$$\Phi = \frac{n_c}{S_c}\int_{V_c} \mathbf{A}\cdot\mathbf{n}_s dv \tag{4}$$

where

n_c, S_c are the number of turns and cross sectional area of the coil respectively;

$\mathbf{n}_s$ is the unit vector along the direction of the exciting current , and

V_c is the coil area.

In the simulation with current source, the exciting current I_0 is represented by using the exciting current density $\mathbf{J}_0$ as

$$\mathbf{J}_0 = \frac{n_c}{S_c} I_0 \mathbf{n}_s \tag{5}$$

So the inter-linkage flux of the exciting coil is re-written by $\mathbf{J}_0, I_0, \mathbf{A}$

$$\Phi = \int_{V_c} \frac{1}{I_0}\mathbf{A}\cdot\mathbf{J}_0 dv \tag{6}$$

Then, the induced primary voltage in each coil at time t can be determined as:

$$V_i(t) = \frac{\Phi(t) - \Phi(t-\Delta t)}{\Delta t} \tag{7}$$

From this result, the absolute value of the impedance of the equivalent circuit is calculated as:

$$|Z_i| = \frac{|V_i|}{|I_i|} \tag{8}$$

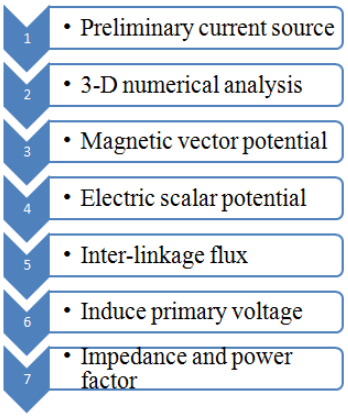

Fig. 4. Flowchart of impedance calcualation

And the power factor is calculated by using the phase difference between the input current and the back EMF (9). The details of this calculation flowchart can be seen in Fig. 4.

$$p.f. = \cos\Delta\theta \tag{9}$$

While the power factor is determined by the impedance value, the efficiency can be calcualted from output power and secondary loss as:

$$\eta = \frac{F_x v}{F_x v + P_2} \tag{10}$$

C. Eddy Current Illumination for Transverse Edge-effect

As seen in Fig. 2, the pattern of the eddy current in the secondary reaction plate is described through 3-D numerical analysis. In order to estimate the influence of the transverse edge effect, the authors have considered the distribution of the eddy current of z-component in comparison with the total eddy current along z-direction of secondary reaction plate through ratio as:

$$\varepsilon_i = \frac{\iint_{S_k} |i_{z(i)}|\,dxdy}{\sqrt{(\iint_{S_k} |i_{x(i)}|\,dydz)^2 + (\iint_{S_k} |i_{y(i)}|\,dxdz)^2 + (\iint_{S_k} |i_{z(i)}|\,dxdy)^2}} \tag{8}$$

where

$i_{x(i)}, i_{y(i)}, i_{z(i)}$ are eddy current density along *x*, *y* and *z* components at elements along *z*-component.

As a result, we can get the arithmetic mean of ε_i along *z*-direction, so it can be used for the indicator of the transverse edge-effect occurring in LIM. If its value is close to 1, it means that the eddy current is distributed along z-direction and the influence of edge-effect is reduced. The closer the ε_i value is to 1, the better the edge-effect decreases.

IV. Numerical Analysis and Experimental Results

By using the numerical analysis method described above, the performance of LIM has been evaluated among the 2-D analysis (without end & edge-effect), 3-D analysis (with end & edge-effect) and the experiment, Fig. 5. The significant difference in air gap magnetic flux distribution can be seen between 2-D and 3-D analysis, as in Fig. 6. The non-uniform

and influence of lateral region of the flux have strong effect on the thrust and impedance calculation in 3-D analysis.

Fig. 7 is the distribution of magnetic flux along x-direction at $z = 0$ obtained by 3-D analysis at 2 poles along travelling direction in the experiment. With the same analysis conditions, copper reaction plate and 21Hz slip frequency, it is found that the error between numerical analysis and experiment is acceptable.

In addition, in case of copper reaction plate, the absolute value of the impedance and power factor obtained from voltage and current measurement is compared with the 3-D transient analysis results. Due of the restriction in experiment conditions, all of the experiments with different primary frequencies are taken at the same slip frequency of 1.0.

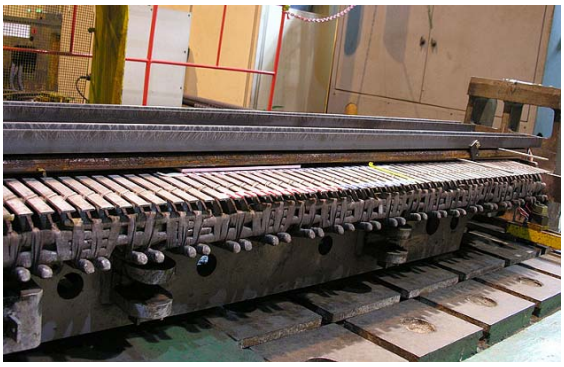

Fig. 5. Experimental equipment in real LIM system

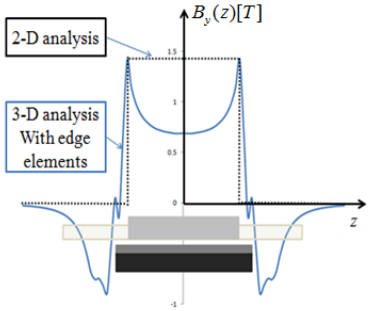

Fig. 6. Distribution of air gap magnetic flux along z-direction in 2-D and 3-D analysis

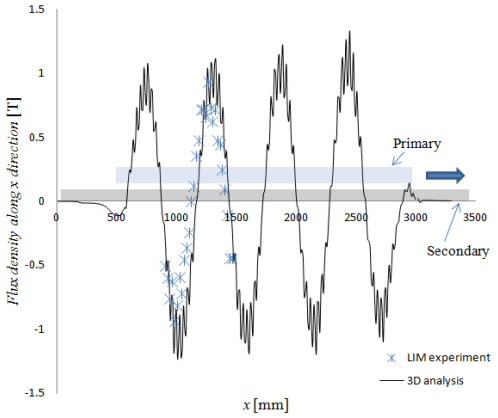

Fig. 7. Flux density along x-direction in 3-D analysis and experiment

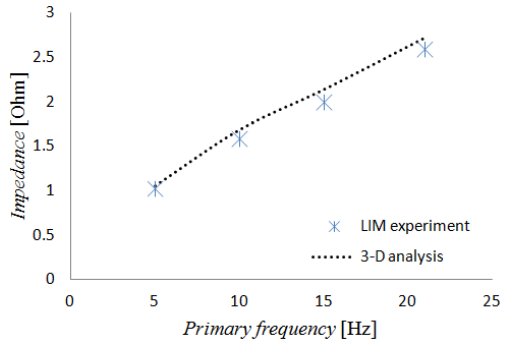

(a) Absolute value of impedance and primary frequency relation

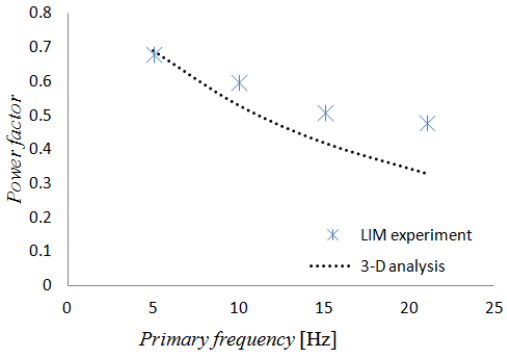

(b) Power factor and primary frequency relation

Fig. 8. 3-D analysis and experiment results

While the absolute value of the impedance and the power factor in 3-D analysis with current source are determined by the calculation method described above, these values are obtained from voltage and current measurement in experiment. There is no plain difference between simulation and experiment in the absolute value of the impedance, Fig 8(a), but in case of power factor, the difference becomes larger when the primary frequency increases, Fig 8(b). This can be explained as: since there are only the conductor plate and iron plate in the secondary side in LIM, and because of the strong influence of skin effect, magnetic saturation occurs easily, especially in high primary frequency, which affects the physical properties such as permeability and conductivity. Thus, it is necessary to consider the non-linear characteristics with magnetic saturation. However, it is impossible because of the complex approximation in LIM analysis. Therefore, in this paper, permeability and conductivity of secondary back iron are setted at a constant value as shown in Table II, and the power factor seems to decrease as a result of proportional relation.

V. PERFORMANCE WITH DIFFERENT DESIGNS OF SECONDARY REACTION PLATE

A. Different Designs of Secondary Reaction Plate for High Performance Consideration

With the same primary design, the performance of LIM directly depends on the secondary reaction plate design and its materials. Moreover, in order to reduce the influence of the non-continuity of the electromagnetic field, various shapes

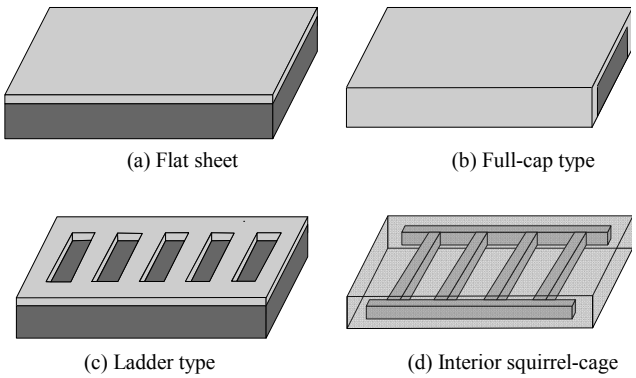

Fig. 9. Various configuration of secondary reaction plate

of the secondary part should be considered. However, because of the restriction of the real experiment conditions, analytical methods and numerical simulation are generally used to analyze the performance in each case. Fig. 9 shows the various configurations of the secondary reaction plate.

B. Performance of LIM with Different Caps

In the design of LIM for urban transit with a maximum speed of about 70km/h, this paper concerns the using of difference caps in secondary reaction plate for the evaluation of the LIM performance (motor characteristics) including thrust, power factor, efficiency and edge-effect. The overhang length c should be large, 20 to 40 cm, with the cap height h_c in order to reduce the edge-effect and consider the cost of the secondary material, Fig. 10.

Together with the next generation of LIM for linear metro in Japan, this paper considers the full cap model, $c = 30, h_c = 27, l_c = 30$ mm. The performance of this model with different slip frequencies near the rated slip frequency is described in comparison with the flat-shaped model in 2-D and 3-D analysis.

Fig. 11 is the distribution of the eddy currents through the ratio between the eddy current of z-component and the total eddy current along z-direction in secondary plate and air gap flux density along z-component through ε_i, as described in (8). It can be seen that in full cap model, that the eddy current under stack lengh of primary in z-component increases means the influence of x-component eddy current decreases. In addition, magnetic flux density at the air gap along z-component is more balanced in the full cap model. The difference of the magnetic flux from the center to the end of the secondary reaction plate is reduced causing the edge-effect reduced due to using full cap for secondary reaction plate.

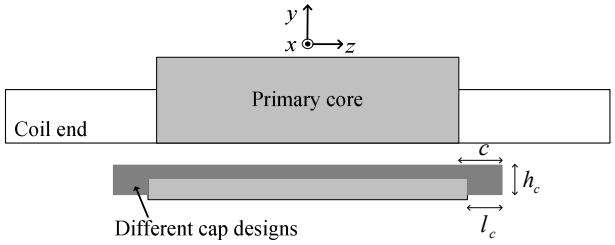

Fig. 10. Lateral view of the model with the different secodary reaction plate

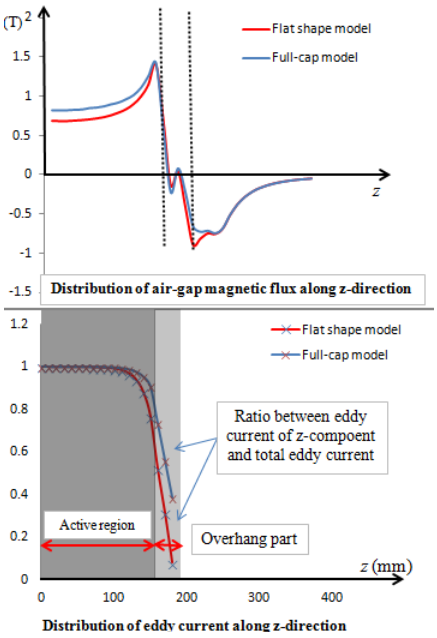

Fig. 11. Distribution of eddy current (up) and air-gap flux densigy (down) along z-component in different cap models

Other parameters including thrust, power factor, secondary loss and efficiency are expressed in Fig. 12. The performing results show that using cap for secondary conductor is a significant design to reduce eddy current loss in secondary part; hence, the thrust and efficiency of LIM are improved. In addition, with the decrease of magnetizing inductance, especially at high speed, this design is a good design in term of power factor improvement.

VI. CONCLUSION

In this paper, the 3-D numerical electromagnetic analysis for the effect of the construction of the secondary reaction plate on the characteristics of LIM is described in designing a new LIM for linear metro systems. The reliability of this method has been tested and approved by comparing with the experimental results. By using this method, it is possible to determine the characteristics of LIM with high accuracy through a number of tests that cannot be realized under normal conditions. The 3-D numerical analysis has proved the significant result for obtaining higher thrust and reducing primary input concerning the usage of cap for secondary reaction plate. Since the construction of secondary reaction plate is an important design factor from the viewpoint of safety characteristics, and cost of building and performance, the method proposed in this paper can be used to find the optimal design of LIM for linear metro system.

In future work, other designs of secondary reaction plate as well as the saturation of back iron will be considered by using 3-D numerical analysis and this calculation method.

ACKNOWLEDGMENT

The authors gratefully acknowledge the support of Hitachi, Ltd and Japan Subway Association (JSA) to this work.

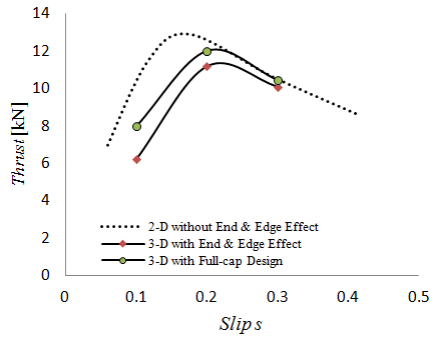

(a) Thrust characteristic

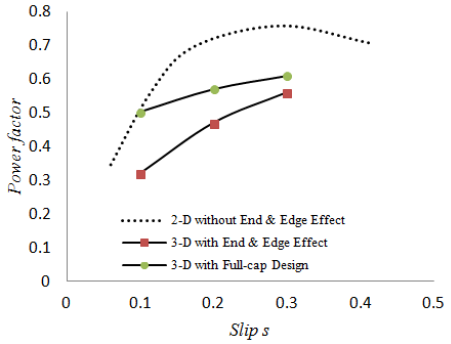

(b) Power factor characteristic

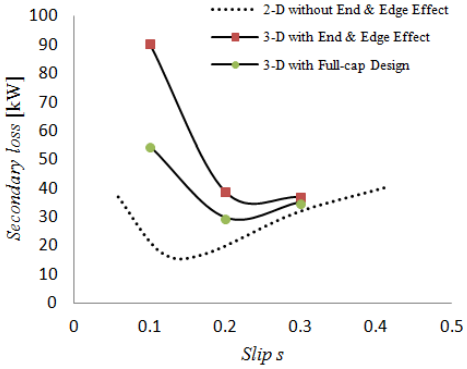

(c) Secondary loss characteristic

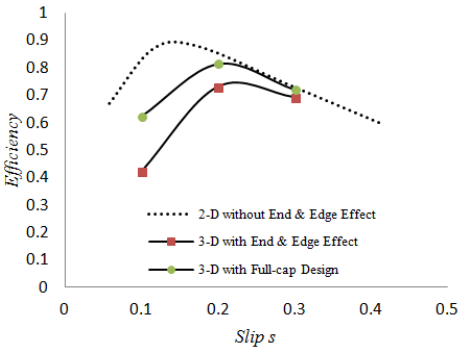

(d) Efficiency characteristic

Fig. 12. Varieties characteristics of LIM concerning secondary construction

REFERENCES

[1] E. Isobe, J. Cho, I. Morihisa, T. Sekizawa, R. Tanaka, "Linear metro transport systems for the 21st century,"

[2] S. Yamamura, "Theory of linear induction motor," The University of Tokyo Press, 1972.

[3] T. Koseki, "Flux sysnthesizing linear induction motor, " The University of Tokyo, PhD. Thesis, 12.1991.

[4] Y. Nozaki, "Identification of linear induction motor plant model with significant consideration of end-effect," The University of Tokyo, PhD. Thesis, 2007. 12 (In Japanese)

[5] N. V. Cuong, Y. Yamamoto, and T. Koseki, " 3D numerical analysis for impedance calculation and high performance consideration of linear induction motor for rail-guided transportation, " Proceedings of AES 2013, Sharjah-UAE, pp. 62-67, 2013.

[6] Three-dimensional non-linear dynamic magnetic field analysis with ELF/MAGIC
URL: http://www.elf.co.jp/product/elfmagic.html

[7] S. G. Lee, H. W. Lee, S. H. Ham, C. S. Jin, H. J. Park and J. Lee, "Influence of the construction of secondary reaction plate on the transverse edge effect in linear induction motor, " IEEE Trans. Magn., Vol. 45, No. 6, pp.2815-2818, June 2009.

[8] T. Yamaguchi, Y. Kawase, M. Yoshida, and Y. Ohdachi, "3-D finite element analysis of a linear induction motor, " IEEE Trans. Magn.,vol.37, no. 5, pp. 3668-3671, Sep. 2001.